Computational and Experimental Study on the Interaction of Terbium (III) and Ytterbium (III) Complexes Containing 1,10-phenanthroline with Bovine Serum Albumin

Aramesh Boroujeni, Zahra*[+]

Department of Chemistry, University of Isfahan, Isfahan, I.R. IRAN

Jahani, Shohreh

Noncommunicable Diseases Research Center, Bam University of Medical Sciences, Bam, I.R. IRAN

ABSTRACT: *In this work, the interaction of two synthesized complexes $[Tb(phen)_2Cl_3.OH_2]$ and $[Yb(phen)_2Cl_3.OH_2]$ (phen is 1,10-phenanthroline) with bovine serum albumin (BSA) were studied by UV-Vis, fluorescence, and molecular docking examinations. The experimental data indicated that these lanthanide complexes have a high binding affinity with BSA by effectively quenching the fluorescence of BSA via the static mechanism. The binding parameters, the type of interaction, the value of resonance energy transfer, and the binding distance between complexes and BSA were estimated from the analysis of fluorescence measurements and Förster theory. The thermodynamic parameters suggested that van der Waals interactions and hydrogen bonds play an important role in the binding mechanism. While the energy transfer from BSA molecules to these complexes occurs with high probability, the binding constants showed that the binding affinity ranked in the order Tb-complex > Yb-complex, which has been related to the radius of Ln^{3+} ion. Also, the results of competitive experiments and molecular docking calculations assessed the microenvironment residues around the bound mentioned complexes and represent site 3 of BSA, located in subdomain IB, as the most probable binding site for these complexes. The computational results kept in good agreement with experimental data.*

KEYWORDS: *Lanthanide complex; Bovine serum albumin; Binding interaction; Fluorescence spectroscopy; Molecular docking.*

INTRODUCTION

Lanthanide complexes with organic ligands often show efficient fluorescence emission. This effect is the result of the strong absorption of the organic ligands and efficient intramolecular energy transfer from the excited triplet state of ligands to the emitting level of rare-earth atoms (antenna effect). The emission of light from rare-earth ions arises

***** *To whom correspondence should be addressed.*
+ *E-mail*: *zaramesh.boroujeni@gmail.com*
1021-9986/2022/1/58-70 13/$/6.03

from f–f transitions, which result in narrow emission bands, significant stokes shift, and long luminescence lifetime. This makes rare-earth ions very attractive probes for the selective detection of proteins in a variety of biological and chemical applications [1-5]. Among Ln(III) ions, Tb^{3+} has intense, long-lived, and line-like emission in the visible region that enables them to be promising in applications from display devices to biological assays [6]. Moreover, it was found that lanthanide complexes have several essential roles in the medicinal and pharmaceutical field, including anticoagulants, anti-inflammation, and arteriosclerosis-preventing actions [7-11].

Since lanthanide complexes show a variety of biological applications, some studies have investigated the binding properties of these complexes with serum albumin, which is the most abundant serum protein in the body of all vertebrates [12-19]. This protein contributes to the apparent solubility of hydrophobic compounds in blood plasma and modifies their transportation to target tissues. Moreover, Bovine Serum Albumin (BSA) has emerged as a transporter for therapeutic and diagnostic agents and it binds to a variety of substrates, involving fatty acids, amino acids, metal cations, hormones, and various therapeutic drugs. It has been revealed that the distribution, the free concentration, and the metabolism of several drugs can be considerably altered as a result of their bindings to bovine serum albumin [20, 21]. The crystallographic analyses of BSA disclosed that this protein contains three similar α-helical domains (I, II, and III), each of which comprises two subdomains (A and B). This protein has three binding sites 1, 2, and 3, which are located in sub-domains IIA, IIIA, and IB, respectively [22].

In the present paper, in continuation of our previous work [23-27], here we attempted to introduce Tb^{+3}, Yb^{+3} complexes with phen ligand as a new probe to BSA. Thus, based on the potential biological properties of lanthanide complexes, the interaction of Tb(III) and Yb(III) complexes with BSA has been widely investigated by using fluorescence spectroscopy, UV–Vis, and molecular docking methods. This study provides valuable information about the binding modes and binding affinities of these lanthanide complexes in the binding site of BSA. It determines the role of this serum protein in the transporting of these complexes in the blood.

EXPERIMENTAL SECTION

Reagents and Instrumentations

BSA (free fatty acid fraction V, purity > 97%) was obtained from Sigma chemical company and stored at 4 ℃. All of the other reagents and solvents were purchased from Merck & Aldrich chemical companies. All used materials were in analytical grade and used without further purification. All experiments were carried out in Tris–HCl buffer (50 mM NaCl–5 mM Tris-HCl, pH 7.20). Fluorescence measurements were carried out by RF-5000 (Kyoto, Japan) spectrofluorimeter, equipped with 1.0 cm quartz cells and a thermostat bath, which kept the temperature constant within ±0.1 °C. The UV–Vis spectra were recorded on a JASCO (V-670) spectrophotometer with a 1 cm optical-path quartz cell.

Synthesis and characterization of the complexes

The Tb complex and Yb complex were synthesized concerning the literature method [28]. An ethanolic solution of 1,10-phenanthroline was added to a hot ethanolic solution of the hydrated metal chlorides (100 mg) in a 2:1 mole ratio. The reaction mixtures were refluxed for 8 hours to complete the reaction. Then, the products were filtered, washed several times with ethanol and dichloromethane, and dried in a vacuum. The products were characterized by using CHN, FT-IR, and UV-Vis techniques. The results of the characterization are as follow:

Anal. Calc. for $C_{24}H_{16}Cl_3N_4OTb$ (641.4 g/mol): C, 44.9%; H, 2.49%; N, 8.73%. Found: C, 45.8%, H, 2.52%; N, 8.67 %, IR (KBr, cm^{-1}): ν(OH) = 3213, ν(C=N) = 1623; ν(C=C) = 1464; ν(C–H) = 729-873, ν(Tb—N) = 650-450, ν(Tb—O) = 570-400. UV–Vis Absorption (in H_2O): 230, 271 nm.

Anal. Calc. for $C_{24}H_{16}Cl_3N_4OYb$ (655.55 g/mol): C, 43.93%; H, 2.44%; N, 8.54%. Found: C, 45.1%, H, 2.49%; N, 8.46 %, IR (KBr, cm^{-1}): ν(OH) = 3214, ν(C=N) = 1602 cm^{-1}; ν(C=C) = 1427-1537 cm^{-1}; ν(C–H) = 725-876 cm^{-1}, ν(Yb—N) = 651-450, ν(Yb—O) = 570-400. UV–Vis Absorption (in H_2O): 230, 270 nm.

Preparation of stock solutions

The stock solution of BSA (10 mg/mL) was prepared by dissolving BSA in Tris–HCl buffer, pH 7.20. The accurate protein concentration was determined spectrophotometrically using the molecular absorption coefficient of $\varepsilon_{280\ nm}$ = 44300 $M^{-1}cm^{-1}$ [25]. The protein

stock solutions were kept in at 4 °C and used within four days. These complexes have dissolved in tris buffer completely. The stability of these complexes in an aqueous solution was studied by following the UV–Vis spectrum of Tb-complex and Yb-complex at several incubation times.

BSA binding experiments

The interaction of Tb(III) and Yb(III) complexes with BSA was examined by UV-Vis and fluorescence spectroscopies. Absorption titrations were performed at a constant concentration of BSA (10 μM) by increasing lanthanide complexes concentration (0.5– 6.5 μM), and the corresponding complex solution was used as a reference solution. The fluorescence titrations were performed at a constant concentration of BSA (3.0 μM) while the increasing concentrations of lanthanide complexes (0.5 to 6.0 μM) at four temperatures (λ_{ex}=280, λ_{em}=348 and T=293, 298, 303 and 308 K).

Actually, the complex has an emission in the range of 300-500 nm at an excitation wavelength 270 nm but it's quantum efficiencies were much lower than BSA. However, the intensity emission of the complex is much lower than BSA solution within the mentioned concentration range of this study. The dilution effect (the addition of subsequent volumes of complex to the BSA solution in the cell, which decreases the total concentration of BSA that should be considered in the correction of fluorescence data) and the fluorescence intensity of the complex are two factors that have been considered for modification of fluorescence titration data. For the second correction, the Inner Filter Effect (IFE) must be considered in the fluorescence spectrum measurements. Generally, the fluorescence intensity with IFE can be corrected by the following equation [29, 30]:

$$F_{cor} = F_{obs} \cdot 10^{\frac{A_1 + A_2}{2}} \quad (1)$$

Where F_{cor} is the corrected fluorescence intensity and F_{obs} is the observed fluorescence intensity in the experiment, A_1 and A_2 are the totality of the absorbance of all components at the excitation wavelength (λ) and the emission wavelength (λ), respectively. Thereby, fluorescence titration data were corrected by considering these negligible values.

Competitive experiments for BSA

To identify the binding site of Tb(III) and Yb(III) complexes on BSA, competitive fluorescence binding tests have been carried out in the absence and presence of the famous ligands, phenylbutazone, ibuprofen, and hemin as the site I marker, site II markers, and site III markers, respectively [25]. In the typical titration experiment, the concentration of the lanthanide complex varied from 0.5 to 6.0 μM, and the concentration of BSA and site marker was stabilized at 3 μM and 0.3 μM, respectively. For the running of this experiment, the specified amounts of the stock solution of Tb(III) and Yb(III) complexes (100 μM) were sequentially added to the BSA and BSA- site marker solutions. An excitation wavelength at 280 nm was selected, and fluorescence spectra were recorded in the range of 300– 450 nm.

Docking protocol

In this experiment, Autodock4.2.6 was used for docking calculations by a semi-flexible docking method. During all docking processes, BSA was kept rigid while all the complex bonds of complexes were set free. The crystal structure of BSA (PDB ID: 3v03) was taken from the Brookhaven Protein Data Bank (BPDB). The 3D structure of the Tb-complex and Yb-complex were optimized by using the Becke-3-parameter Lee–Yang–Parr hybrid Density Functional Theory (DFT) at the 6–31 G** basis set level by employing the quantum chemistry software ORCA [31, 32]. For this study, molecular docking was performed in the different regions of BSA (three active sites of BSA) to search for the most stable complex [33, 34]. The grid map with 0.375 Å spacing and 80 × 80 × 80 points was generated. Then, 200 separate docking calculations were done, and the docking calculation contained the maximum number of 25,000,000 energy evaluations using the Lamarckian genetic algorithm local search method [35].

RESULTS AND DISCUSSION

UV-Vis spectroscopy measurements

The performance of a drug is considerably influenced by the degree to which the drug binds to proteins in the plasma of blood. Absorption spectroscopy is an important technique to explore changes and also complex formations in protein [36]. It can be observed in Fig. 1 that there are two electronic absorption bands: one is a strong band in ~ 212 nm attributed to reflected the BSA framework confirmation, other is a weak absorption band in ~ 280 nm reflected the π→π* transition of the aromatic amino acids (for example Tyr, Trp, and Phe) [37]. It was clear that

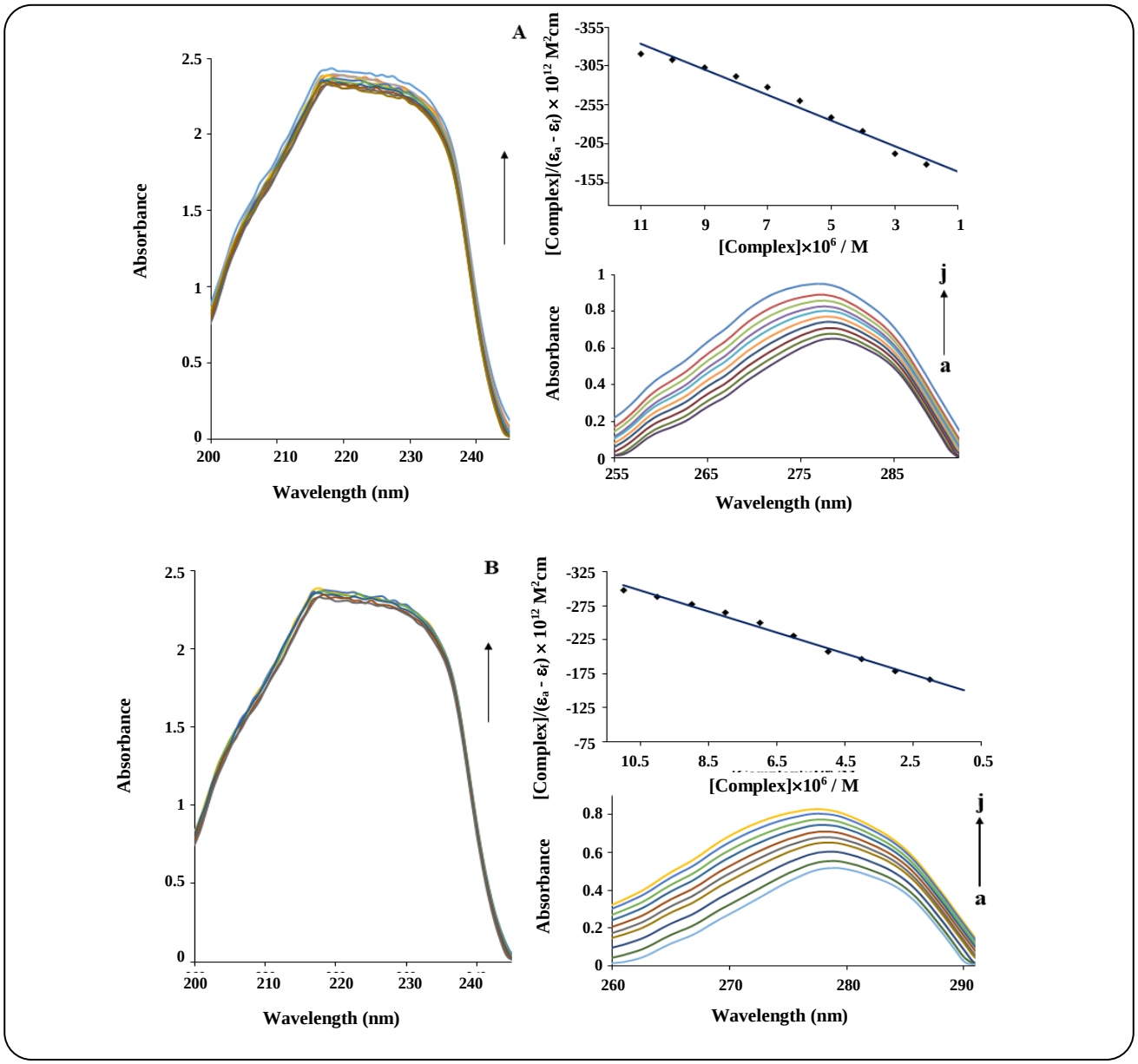

Fig. 1: Absorption spectra of BSA in the absence and in the presence of various concentrations of (A) Tb(III) complex (B) Yb(III) complexes, [Complex] = 0– 4.5 µM (a=0, b= 0.5, c= 1.0, d= 1.5, e= 2.0, f= 2.5, g= 3.0, h= 3.5, i= 4.0, j= 4.5 µM), [BSA] = 10 µM. T= 298 K. Inset is the plot of [Complex]/ (ε_a-ε_f) versus [Complex].

the intensity of absorption of BSA (10 µM) increased with the addition of Tb(III) and Yb(III) complexes (0.5– 6.0 µM). However, if the maximum band position does not change at a fixed concentration of BSA, displaying that the interaction of complexes increased the absorption of BSA without changing in the local dielectric environment of its residues (Trp and Tyr). To determine the binding constant, K_b equation 1 was used for fitting the data [38].

$$[Q]/(\varepsilon_a - \varepsilon_f) = [Q]/(\varepsilon_b - \varepsilon_f) + 1/K_b(\varepsilon_b - \varepsilon_f) \quad (2)$$

Where ε_a, ε_f, and ε_b have corresponded to the apparent extinction coefficient (A_{obsd}/ *[BSA]*), the extinction coefficient for the free BSA in solution, and its completely complex-bound combination, respectively, and *[Q]* is the concentration of complex. K_b was given by the plots of [*complex*]/ (ε_a - ε_f) *vs.* [*complex*] from the ratio of the slope to the y-intercept (insert Fig. 1). The K_b values for terbium and ytterbium complexes were found to be 3.13 × 10^5 and 2.07 × 10^5 M^{-1}. These results suggest that the interaction of these lanthanide complexes with BSA is a non-intercalative binding mode.

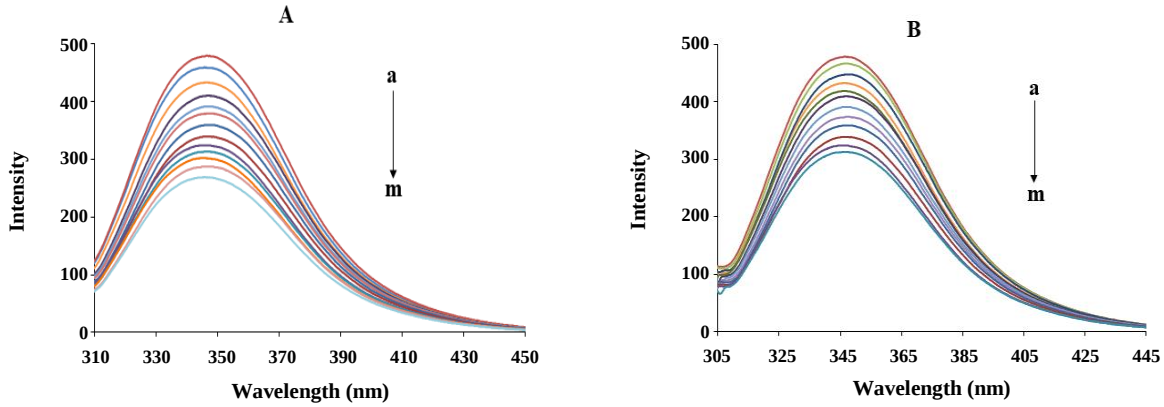

Fig. 2: Fluorescence emission spectra of BSA in the absence and presence of various concentrations of (A) Tb(III) complex (B) Yb(III) complex, [BSA] = 3 µM and [Complex] = 0 to 6.0 µM (a=0, b= 0.5, c= 1.0, d= 1.5, e= 2.0, f= 2.5, g= 3.0, h= 3.5, i= 4.0, j= 4.5, k=5.0, l= 5.5, m= 6.0 µM, T= 298 K and λ_{ex}= 280 nm, pH= 7.2).

Fluorescence spectroscopy

Luminescence titration with complexes

Fluorescence spectroscopy can supply necessary information on the interaction of small molecules with proteins, such as the binding mechanism, binding mode, and so on [39]. The emission spectra of BSA in the presence of various amounts of Tb(III) and Yb(III) complexes at 298 K are shown in Fig. 2. By considering these figures, the fluorescence intensity of BSA was gradually decreased with the increasing concentration of these lanthanide complexes, which indicated the ability of these complexes for quenching of intrinsic fluorescence of BSA and the occurrence of their binding interaction. A valuable feature of the intrinsic emission of proteins is the high sensitivity of protein fluorophores (especially tryptophan) to their local environment. Although the changes in the fluorescence spectra of protein are commonly in response to protein conformational transitions, subunit association, or substrate binding [40], the absence of any blue or redshifts in the maximum emission wavelength may be represented the small alteration in the microenvironment of protein fluorophore residues due to the binding of these lanthanide complexes.

Temperature effect on quenching efficiency

The titration data were obtained from the interaction study of BSA with Tb and Yb complexes at different temperatures (293, 298, 303, and 308 K) were fitted into the Stern–Volmer equation (Eq. (3)) [26]:

$$\frac{F_0}{F} = 1 + K_{SV}[Q] = 1 + k_q \tau [Q] \quad (3)$$

Where F_0 and F are the fluorescence emission intensities of BSA in the absence and presence of the quencher (lanthanide complexes), respectively, [Q] is the concentration of quencher, k_q is the quenching rate constant of the biomolecule, τ_0 (10^{-8} s [41]) is the average lifetime of the fluorescent substance without any quencher and K_{SV} is the Stern–Volmer quenching constant, which can be considered as a measure for the efficiency of fluorescence quenching by lanthanide complexes. Eq. (3) was applied to determine K_{SV} by linear regression of a plot of F_0/F *vs.* *[Q]*. The K_{SV} and k_q of BSA by mentioned complexes at different temperatures were obtained, and the results are shown in Fig. 3 and Table 1. From the K_{SV} values, it is obvious that the Tb complex is a stronger quencher than the Yb complex for BSA. As seen in Fig. 3, the Stern-Volmer plots were linear with a high correlation coefficient.

Two kinds of quenching processes are known: dynamic and static. Dynamic quenching requires contact between the excited luminophore and the quencher, while static quenching refers to luminophore quencher complex formation. In general, static and dynamic quenching can also be discerned by their differing dependence on temperature and excited-state lifetime. For dynamic quenching, higher temperatures can cause a collision to increase, so the bimolecular quenching constant can be enhanced by increasing the temperature. In contrast, in static quenching, increased temperature is likely the result

Table 1: The Stern-Volmer constant K_{SV}, biomolecular quenching rate constant k_q, number of substantive binding sites n, the binding constant K_b and thermodynamic parameters for the binding of Tb- complex and Yb- complex with BSA at different temperatures.

Complex	T(K)	$K_{SV} \times 10^{-4}$ (M^{-1})	$k_q \times 10^{-12}$ ($M^{-1}s^{-1}$)	n	$K_b \times 10^{-5}$ (M^{-1})		ΔG° (kJ/mol)	ΔH° (kJ/mol)	ΔS° (J/mol.K)
					UV	Fluorescence			
	293	8.27 ± 0.03	8.27 ± 0.03	117		6.46 ± 0.04	-32.59 ± 0.04		
Tb(III)	298	7.09 ± 0.02	7.09 ± 0.02	1.16	3.13 ± 0.03	4.91 ± 0.02	-32.46 ± 0.05	-60.08 ± 0.01	-93.49 ± 0.03
	303	6.59 ± 0.05	6.59 ± 0.05	1.12		2.82 ± 0.04	-31.61 ± 0.03		
	308	3.88 ± 0.02	3.88 ± 0.02	1.13		2.04 ± 0.03	-31.31 ± 0.02		
	293	7.21 ± 0.05	7.21 ± 0.05	1.16		5.75 ± 0.04	-32.31 ± 0.04		
Yb(III)	298	6.51 ± 0.06	6.51 ± 0.06	1.14	2.07 ± 0.05	3.71 ± 0.02	-31.77 ± 0.02	-68.13 ± 0.06	-122.34 ± 0.04
	303	3.97 ± 0.04	3.97 ± 0.04	1.13		2.04 ± 0.04	-30.80 ± 0.03		
	308	2.57 ± 0.02	2.57 ± 0.02	1.14		1.54 ± 0.03	-30.60 ± 0.05		

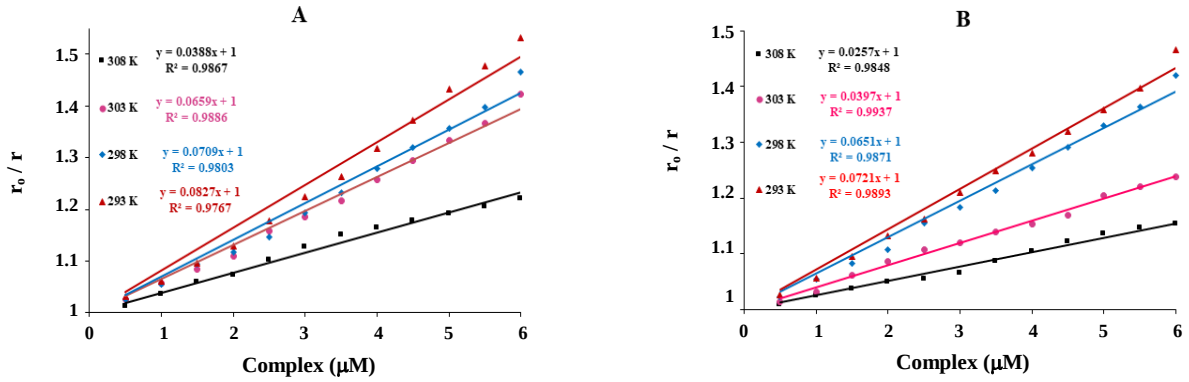

Fig. 3: Stern–Volmer curves for the binding of lanthanide complexes with BSA at 293, 298, 303, and 308 K ((A) Tb(III) and (B) Yb(III) complexes).

of the decrease in the stability of the complex, which will cause the fluorescence quenching constants to decrease [42]. For the reported values of K_{SV} in Table 1, the decreasing of K_{SV} with increasing temperature represents the static quenching mechanism for these lanthanide complexes. Moreover, the maximum dynamic quenching constant of several known quenchers with a biopolymer is around $2.0 \times 10^{10}\ M^{-1}s^{-1}$ [43]; then, the k_q values obtained for these complexes were higher (in the range of 10^{12} $M^{-1}s^{-1}$). Thereby, the static mechanism is responsible for the protein–lanthanide complex binding.

Binding constants and binding sites

To evaluate the interaction between BSA and these lanthanide complexes, the binding constant (K_b) and the binding stoichiometry (n) were determined from the analysis of spectrofluorometric titration data by the following equation [25]:

$$\log \frac{F_0 - F}{F} = \log K_b + n \log [Q] \qquad (4)$$

The binding constant K_b and n are obtained by plotting $\log[(F_0\text{-}F)/F]$ versus $\log [Q]$. The linear equations of $\log[(F_0\text{-}F)/F]$ versus $\log [Q]$ at different temperatures are shown in Fig. 4, and the corresponding estimated parameters are reported in Table 1. The number of binding sites (n) is close to 1 revealed that there was just a single binding site for BSA towards these complexes. The K_b at 298 K for Tb and Yb complexes were found to be 4.91×10^5 and 3.71×10^5 M^{-1}, respectively. The values of binding

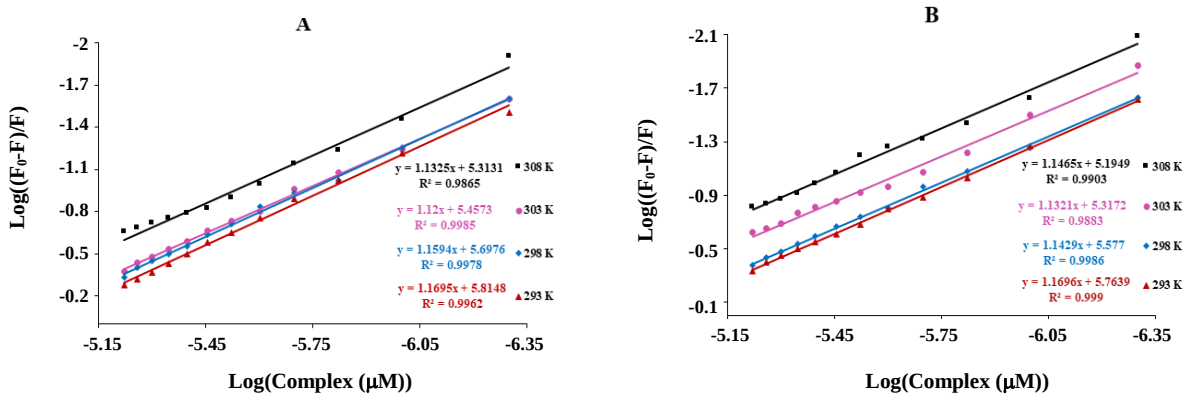

Fig. 4: Plots of log((F₀-F)/F) versus log([Complex]/μM) for the binding of (A) Tb (B) Yb complexes with BSA at 293, 298, 303, and 308 K.

constant indicates the remarkably high affinity of BSA to these complexes and the following order for binding affinity: Tb-complex > Yb-complex.

Also, the obtained data were compared with similar complexes (such as Yb(III) and Dy(III) containing 2,2'-bipyridine ligand with K_b at 298 K 6.45 $\times 10^5$ M^{-1} [26] and 2.81$\times 10^5$ [25] M^{-1}, respectively) indicated that these complexes have high binding affinities with BSA comparable with similar compounds.

Thermodynamic parameters and binding forces

In general, the interaction forces between biomolecules and small molecules like drugs involve several bonds such as hydrophobic forces, hydrogen bonds, van der Waals interactions, and electrostatic forces [44]. The relationship between main binding forces and thermodynamic parameters was concluded by Ross and Subramanian [45] as follows: (1) $\Delta H > 0$ and $\Delta S > 0$ suggest a hydrophobic forces; (2) $\Delta H < 0$ and $\Delta S > 0$ indicates electrostatic force; and (3) $\Delta H < 0$ and $\Delta S < 0$ reflect the van der Waals interactions and hydrogen bonds. The values of the enthalpy change (ΔH) and the entropy change (ΔS) can be obtained from the van't Hoff equation [46]:

$$\ln K_b = -\frac{\Delta G^\circ}{RT} = \frac{\Delta H^\circ}{R}\left(\frac{1}{T}\right) + \frac{\Delta S^\circ}{R} \quad (5)$$

$$\Delta G^\circ = \Delta H^\circ - T\Delta S^\circ \quad (6)$$

Where K_b is the binding constant at the different temperatures, R is the gas constant, and T is the absolute temperature. By plotting lnK_b versus 1/T (Fig. 5), the values

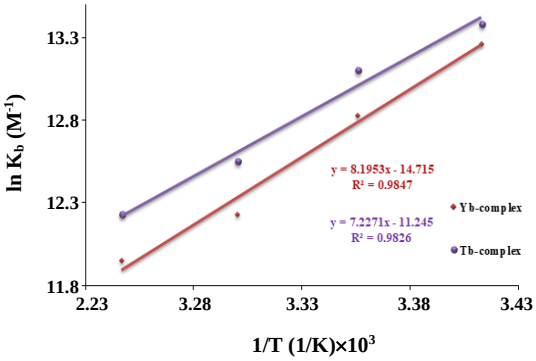

Fig. 5: van't Hoff plot for the binding of lanthanide complexes with BSA.

of ΔH° and ΔS° were determined from the slope and intercept of this plot. The thermodynamic parameters for the interaction of BSA to lanthanide complexes are summarized in Table 1 and represent the negative values for both ΔH° and ΔS°. The negative sign of ΔG° values revealed a spontaneous interaction process. Also, the negative sign of ΔH° and ΔS° indicated the van der Waals interactions and hydrogen bonds as the main binding forces in complex formation.

Energy transfer between lanthanide complexes and BSA

Fluorescence Resonance Energy Transfer (FRET) is a reliable technique for studying interactions of the protein with compounds and measuring the molecular distance in various macromolecular systems. FRET occurs whenever the emission spectrum of the donor overlaps with the absorption spectrum of the acceptor that is within 2–8 nm. The overlap of the excitation spectrum of the Tb and Yb

Table 2: The energy transfer efficiency E, overlap integral J, the binding distance to tryptophan residue of protein r and Förster critical distance R_0 upon the interaction of Tb- complex and Yb- complex with BSA ([BSA]= [lanthanide complex] = 3 µM, T= 298 K and λ_{ex}= 280 nm).

Complex	*E*	*J* (cm^3Lmol^{-1}) × 10^{-15}	*r* (nm)	R_0 (nm)
Tb- complex	0.19	4.51	2.82	2.23
Yb- complex	0.21	4.52	2.76	2.23

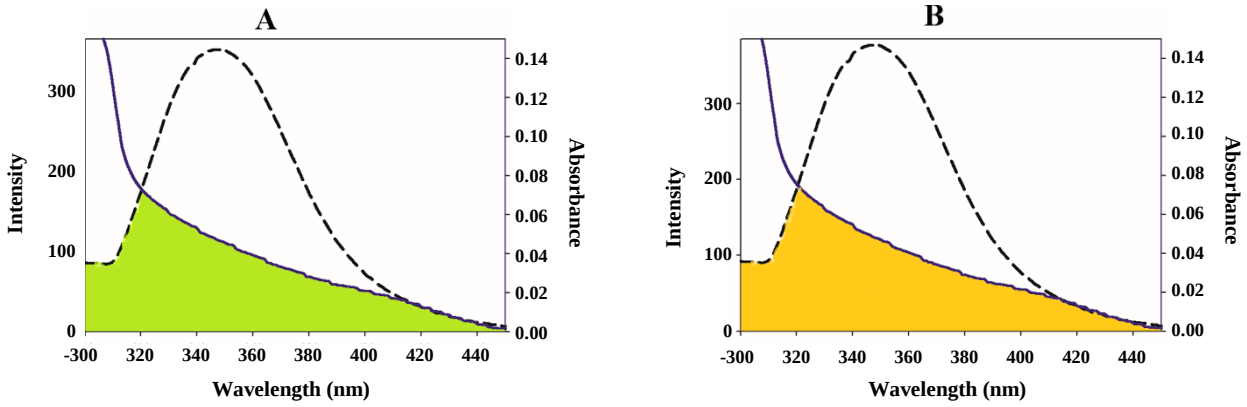

Fig. 6: The overlap of the absorption spectrum (solid lines) (A) Tb (B) Yb complexes and the fluorescence spectrum of BSA (dashed lines). The molar ratio of synthesized complexes to BSA was 1.

complexes with the emission spectra of BSA are shown in Fig. 6. Using FRET, the distance r between the location of these complexes in their binding sites and the fluorophore (Trp-214) of BSA could be calculated by the following equation [47]:

$$E = 1 - \frac{F}{F_0} = \frac{R_0^6}{R_0^6 - r^6} \quad (7)$$

Where *E* is the efficiency of energy transfer between acceptor and donor, F_0 and *F* are the fluorescence intensities of BSA in the absence and presence of the lanthanide complexes, *r* is the distance between acceptor and donor and R_0 is the Förster's critical distance when the transfer efficiency is 50%. The value for R_0 can be calculated using Eq. (8):

$$R_0^6 = 8.79 \times 10^{-25} K^2 N^{-4} \varnothing J \quad (8)$$

Herein, K^2 expresses the spatial orientation factor of dipole and is equal to 2/3, *n* expresses the refracted index of the medium, ϕ is the fluorescence quantum yield of the donor, and *J* is the spectral overlap integral between the fluorescence emission spectrum of the donor and the absorption spectrum of the acceptor. It can be approximated by Eq. (9):

$$J = \frac{\sum F(\lambda)\varepsilon(\lambda)\lambda^4 \Delta\lambda}{\sum F(\lambda)\Delta\lambda} \quad (9)$$

Where $F(\lambda)$ is the fluorescence emission intensity of the fluorescent donor at wavelength λ, and $\varepsilon(\lambda)$ is the molar absorption coefficient of the acceptor at wavelength λ. By considering the following values: K^2 = 2/3, *n* = 1.336 and $\varnothing$ = 0.15 [47]. and using Eqs. (7–9) the values of R_0, *E*, and *r* were estimated and reported in Table 2.

All the *R* and *r* values are in the range of 2–8 nm and it can be realized that $0.5R_0 < r < 1.5R_0$, suggesting a considerable interaction between lanthanide complexes and BSA (Trp-214) and the occurrence of energy transfer phenomena from BSA to these lanthanide complexes with high probability.

Competitive experiments for BSA

Competitive binding tests were performed to elucidate the Tb(III) and Yb(III) complexes binding site on BSA, using phenylbutazone, ibuprofen, and hemin as a site I marker, site II markers, and site III markers, respectively [48- 51].

Table 3: The binding constant of Tb complex and Yb complex with co-solution of BSA and site markers at 298 K.

Complex	System	$K_b \times 10^{-5}\,(M^{-1})$
Tb-complex	BSA	7.41
	BSA-phenylbutazone	4.67
	BSA-ibuprofen	6.02
	BSA-hemin	1.02
Yb-complex	BSA	6.31
	BSA-phenylbutazone	4.67
	BSA-ibuprofen	5.37
	BSA-hemin	0.81

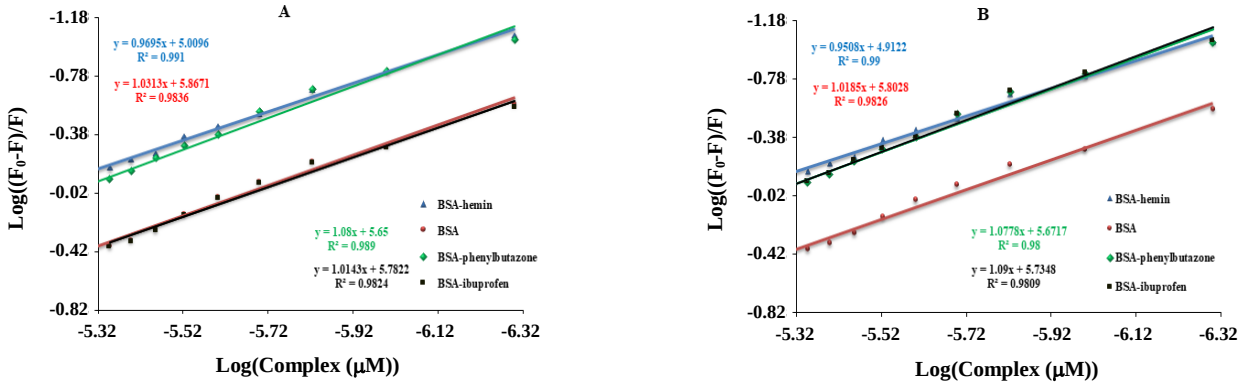

Fig. 7: Effect of site marker to (A) Tb–BSA and (B) Yb–BSA systems, Plots of log((F₀-F)/F) versus log([complex]/μM) in fluorescence study ([BSA]= 3 μM, [site marker] = 0.3 μM, [complex]= 0.5 - 6.0 μM).

In the competitive site experiment, Tb(III) and Yb(III) complexes were regularly added to the solution of BSA and BSA-site marker mixture. After adding the lanthanide complex gradually, the fluorescence intensity of BSA in the present hemin decreased periodically, indicating that the bound lanthanide complex to BSA was obtusely affected by adding hemin. Analysis of fluorescence titration data by using Eq. (4) is indicated in Fig. 7 and Table 3. As shown in Table 3, the K_b value of complex-BSA complex significantly decreased in the presence of hemin. In contrast, the K_b value had a little difference in the presence of ibuprofen and phenylbutazone, indicating that there was a competitive interaction between these complexes and hemin with BSA and the binding site of Tb(III) complex and Yb(III) complex on BSA is consistent with that of hemin on BSA. The competition of these complexes for the occupation of the same binding site represents that the binding of these complexes to BSA is mainly located within site 3 (subdomain IB) of BSA.

Molecular Docking Results

The docking results were clustered based on RMSD between the coordinates of the atoms and were ranked based on binding energies. Finally, the structure with the lowest binding energy and the most cluster members were reported. Molecular docking results illustrated that these complexes showed relatively suitable binding energies (Table 4) and were bound to site 3 of BSA, which is a hydrophobic, L-shaped cavity and is located in subdomain IB. Docking results clarified these complexes have similar binding modes. The detailed interaction of these lanthanide complexes is shown in Fig. 8. This binding site is considerably hydrophobic and PHE36, VAL 40, and TRP134 residues are involved in hydrophobic contacts with lanthanide complexes. Moreover, this complex establishes van der Waals contacts with GLU17, LYS20, LYS131, LYS132, and GLU140 as polar residues. The binding free energy obtained from experimental results at 298 K for Tb(III) and Yb(III) complexes is -7.87 and -7.85 kcal/mol.

Table 4: Binding energies and inhibition constants of investigated complexes for BSA binding site.

Complex	Binding Energy(KCal.Mol^{-1})	K_i (μM)
Tb- complex	-7.87	1.71
Yb- complex	-7.85	1.75

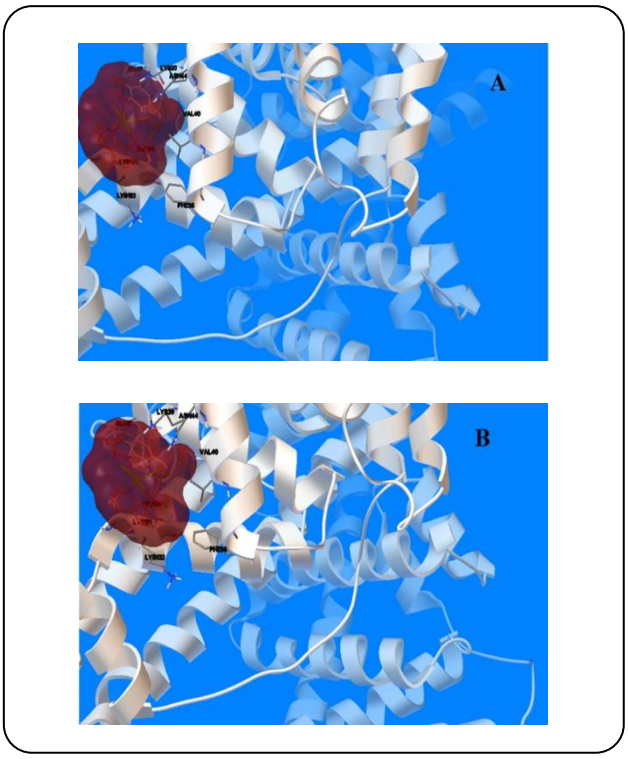

Fig. 8: Detailed view of the interactions between BSA with (A) Tb complex and (B) Yb complex.

The prediction of site 3 (subdomain IB) as the binding site of Yb(III) complex by both docking and experimental according to the Förster theory of non-radiative energy transfer. All approaches employed in this study indicated that the binding affinity to BSA ranked in the order Tb > Yb complexes. These results show that the binding affinity of these complexes has been enhanced with the increasing Ln^{3+} ionic radius (Tb^{3+}>Yb^{3+}). From competitive binding experiments and molecular docking calculations, it revealed that the binding site of these complexes on BSA is in subdomain IB (site 3). The compromising of molecular docking and experimental results could be taken as strong support for the validity of docking results. Briefly, it looks that these complexes can be transported efficiently with BSA in the blood and could be released in tissue targets for their binding affinity values. Moreover, the obtained information from the present study would be helpful for the development of protein probes and new therapeutic reagents for diseases.

CONCLUSIONS

In summary, the present work provided valuable information about the interaction of Tb, and Yb complexes with BSA under simulative physiological conditions. Fluorescence spectroscopic and molecular docking studies were employed in finding the interaction mechanism. The results indicated that the intrinsic fluorescence of BSA was quenched through a static quenching mechanism. These lanthanide complexes are bound to BSA with high affinity, and the interaction process is mainly due to van der Waals interactions and hydrogen bonding. Also, the distance *r* between BSA with Tb and Yb complexes was obtained

Received : Jun. 8, 2020 ; Accepted : Oct. 19, 2020

REFERENCES

[1] Tang K.-Z., Li Y.-F., Tang Y., Liu W.-S., Tang N., Tan M.-Y., Synthesis and Luminescent Properties of the Lanthanide Isothiocyanate Complexes with an Amide-Type Tripodal Ligand, *Spectrochim. Acta, Part A*, **67(3)**: 858-863 (2007).

[2] Jahani S., Noroozifar M., Khorasani-Motlagh M., Torkzadeh-Mahani M., Adeli-Sardou M., In Vitro Cytotoxicity Studies of Parent and Nanoencapsulated Holmium-2, 9-dimethyl-1, 10-phenanthroline Complex Toward Fish-Salmon DNA-Binding Properties and Antibacterial Activity, *J. Biomol. Struct. Dyn.*, **37(17)**: 4437-4449 (2019).

[3] Asadpour S., Aramesh-Boroujeni Z., and Jahani S., In Vitro Anticancer Activity of Parent and Nano-Encapsulated Samarium(III) Complex Towards Antimicrobial Activity Studies and FS-DNA/BSA Binding Affinity, *RSC Adv.*, **10(53)**: 31979-31990 (2020).

[4] Shahraki S., Shiri F., Saeidifar M., Evaluation of in silico ADMET Analysis and Human Serum Albumin Interactions of a New Lanthanum (III) Complex by Spectroscopic and Molecular Modeling Studies, *Inorg. Chim. Acta*, **463**: 80-87 (2017).

[5] Yinhua D., Foroughi M.M., Aramesh-Boroujeni Z., Jahani S., Peydayesh M., Borhani F., Khatami M., Rohani M., Dusek M., Eigner V., The Synthesis, Characterization, DNA/BSA/HSA Interactions, Molecular Modeling, Antibacterial Properties, and *in Vitro* Cytotoxic Activities of Novel Parent and Niosome Nano-Encapsulated Ho(III) Complexes, *RSC Adv.*, **10**(39): 22891-22908 (2020).

[6] Aramesh-Boroujeni Z., Jahani S., Khorasani-Motlagh M., Kerman K., Noroozifar M., Evaluation of Parent and Nano-Encapsulated Terbium(III) Complex Toward its Photoluminescence Properties, FS-DNA, BSA Binding Affinity, and Biological Applications, *J. Trace Elem. Med. Biol.*, **61**: 126564 (2020).

[7] Thompson K.H. Orvig C., Editorial: Lanthanide Compounds for Therapeutic and Diagnostic Applications, *Chem. Soc. Rev.*, **35(6)**: 499-499 (2006).

[8] Fricker S.P., The Therapeutic Application of Lanthanides, *Chem. Soc. Rev.*, **35(6)**: 524-533 (2006).

[9] Li T.-R., Yang Z.-Y., Wang B.-D., Qin D.-D., Synthesis, Characterization, Antioxidant Activity and DNA-Binding Studies of Two Rare Earth(III) Complexes with Naringenin-2-Hydroxy Benzoyl Hydrazone Ligand, *Eur. J. Med. Chem.*, **43(8)**: 1688-1695 (2008).

[10] Aramesh-Boroujeni Z., Aramesh N., Jahani S., Khorasani-Motlagh M., Kerman K., and Noroozifar M., Experimental and Computational Interaction Studies of Terbium(III) and Lanthanide(III) Complexes Containing 2,2′-Bipyridine with Bovine Serum Albumin and Their in Vitro Anticancer and Antimicrobial Activities, *J. Biomol. Struct. Dyn.*, **39(14)**: 5105-5116 (2021).

[11] Aramesh-Boroujeni Z., Asadi Z., Electrochemical Determination Venlafaxine at NiO/GR Nanocomposite Modified Carbon Paste Electrode, *Iranian Journal of Chemistry and Chemical Engineering (IJCCE)*, **40(4)**: 1042-1053 (2021).

[12] Hu Y.-J., Ou-Yang Y., Bai A.-M., Zhao R.-M., and Liu Y., A Series of Novel Rare Earth Molybdotungstosilicate Heteropolyoxometalates Binding to Bovine Serum Albumin: Spectroscopic Approach, *Biol. Trace Elem. Res.*, **136(1)**: 8-17 (2010).

[13] Wang X., Wang X., Wang Y., Guo Z., Terbium (III) complex as a luminescent sensor for human Serum Albumin in Aqueous Solution, *Chem. Commun.*, **47(28)**: 8127-8129 (2011).

[14] Liu E., Zhang H.-x., Interaction of the La (III)–Morin Complex with Human Serum Albumin, *Journal of Solution Chemistry*, **43(8)**: 1402-1413 (2014).

[15] Yousuf I., Bashir M., Arjmand F., Tabassum S., Multispectroscopic Insight, Morphological Analysis and Molecular Docking Studies of CuII-based Chemotherapeutic Drug Entity with Human Serum Albumin (HSA) and Bovine Serum Albumin (BSA), *J. Biomol. Struct. Dyn.*, **37(12)**: 3290-3304 (2019).

[16] Aramesh-Boroujeni Z., Jahani S., Khorasani-Motlagh M., Kerman K., Noroozifar M., Parent and Nano-Encapsulated Ytterbium(III) Complex Toward Binding with Biological Macromolecules, *in Vitro* Cytotoxicity, Cleavage and Antimicrobial Activity Studies, *RSC Adv.*, **10(39)**: 23002-23015 (2020).

[17] Shahraki S., Shiri F., Saeidifar M., Synthesis, Characterization, in Silico ADMET Prediction, and Protein Binding Analysis of a Novel Zinc (II) Schiff-Base Complex: Application of Multi-Spectroscopic and Computational Techniques, *J. Biomol. Struct. Dyn.*, **36(7)**: 1666-1680 (2018).

[18] Shahraki S., Heydari A., New zinc (II) N4 Tetradentate Schiff Base Complex: A Potential Cytotoxic Metallodrug and Simple Precursor for the Preparation of ZnO Nanoparticles, *Colloids and Surfaces B: Biointerfaces*, **160**: 564-571 (2017).

[19] Shahraki S., Shiri F., Majd M.H., Razmara Z., Comparative Study on the Anticancer Activities and Binding Properties of a Hetero Metal Binuclear Complex $[Co(dipic)_2Ni(OH_2)_5]_2H_2O$ (dipic= dipicolinate) with Two Carrier Proteins, *J. Pharm. Biomed. Anal.*, **145**: 273-282 (2017).

[20] Suganthi M., Elango K.P., Spectroscopic and Molecular Docking Studies on the Albumin-Binding Properties of Metal (II) Complexes of Mannich base Derived from Lawsone, *J. Biomol. Struct. Dyn.*, **37(5)**: 1136-1145 (2019).

[21] Singh N., Pagariya D., Jain S., Naik S., Kishore N, Interaction of Copper (II) Complexes by Bovine Serum Albumin: Spectroscopic and Calorimetric Insights, *J. Biomol. Struct. Dyn.*, **36(9)**: 2449-2462 (2018).

[22] Toneatto J. and Argüello G.A., New Advances in the Study on the Interaction of $[Cr(phen)_2(dppz)]^{3+}$ Complex with Biological Models; Association to Transporting Proteins, *J. Inorg. Biochem.*, **105(5)**: 645-651 (2011).

[23] Aramesh-Boroujeni Z., Bordbar A.-K., Khorasani-Motlagh M., Fani N., Sattarinezhad E., Noroozifar M., Computational and Experimental Study on the Interaction of Three Novel Rare Earth Complexes Containing 2, 9-dimethyl-1, 10-phenanthroline with Human Serum Albumin, *J. Iran. Chem. Soc.*, **15(7)**: 1581-1591 (2018).

[24] Aramesh-Boroujeni Z., Bordbar A.-K., Khorasani-Motlagh M., Sattarinezhad E., Fani N., Noroozifar M., Synthesis, Characterization, and Binding Assessment with Human Serum Albumin of Three Bipyridine Lanthanide (III) Complexes, *J. Biomol. Struct. Dyn.*, **37(6)**: 1438-1450 (2019).

[25] Aramesh-Boroujeni Z., Jahani S., Khorasani-Motlagh M., Kerman K., Aramesh N., Asadpour S., Noroozifar M., Experimental and Theoretical Investigations of Dy(III) Complex with 2,2′-bipyridine Ligand: DNA and BSA Interactions and Antimicrobial Activity Study, *J. Biomol. Struct. Dyn.*, **38(16)**: 4746-4763 (2020).

[26] Aramesh-Boroujeni Z., Jahani S., Khorasani-Motlagh M., Kerman K., and Noroozifar M., Evaluation of DNA, BSA binding, DNA Cleavage and Antimicrobial Activity of Ytterbium (III) Complex Containing 2, 2′-Bipyridine Ligand, *J. Biomol. Struct. Dyn.*, **38(6)**: 1711-1725 (2020).

[27] Moradinia E., Mansournia M., Aramesh- Boroujeni Z., Bordbar A.K., New Transition Metal Complexes of 9, 10- phenanthrenequinone p- toluyl Hydrazone Schiff Base: Synthesis, Spectroscopy, DNA and HSA Interactions, Antimicrobial, DFT and Docking Studies, *Appl. Organometal. Chem.*, **33(5)**: e4893 (2019).

[28] Hussain H. and Iftikhar K., 4f–4f Hypersensitivity in the Absorption Spectra and NMR Studies on Paramagnetic Lanthanide Chloride Complexes with 1, 10-phenanthroline in Non-Aqueous Solutions, *Spectrochim. Acta, Part A*, **59(5)**: 1061-1074 (2003).

[29] Shi J.-h., Pan D.-q., Jiang M., Liu T.-T., Wang Q., In Vitro Study on Binding Interaction of Quinapril with Bovine Serum Albumin (BSA) Using Multi-Spectroscopic and Molecular Docking Methods, *J. Biomol. Struct. Dyn.*, **35(10)**: 2211-2223 (2017).

[30] Shi J.-H., Wang Q., Pan D.-Q., Liu T.-T., Jiang M., Characterization of Interactions of Simvastatin, Pravastatin, Fluvastatin, and Pitavastatin with Bovine Serum Albumin: Multiple Spectroscopic and Molecular Docking, *J. Biomol. Struct. Dyn.*, **35(7)**: 1529-1546 (2017).

[31] Neese F., The ORCA Program System, *Wiley Interdiscip. Rev.: Comput. Mol. Sci.*, **2(1)**: 73-78 (2012).

[32] Kondori T., Shahraki O., Akbarzadeh-T N., Aramesh-Boroujeni Z., Two Novel Bipyridine-based Cobalt (II) Complexes: Synthesis, Characterization, Molecular Docking, DNA-Binding and Biological Evaluation, *J. Biomol. Struct. Dyn.*, **39(2)**: 595-609 (2021).

[33] Wang B.-L., Pan D.-Q., Zhou K.-L., Lou Y.-Y., Shi J.-H., Multi-Spectroscopic Approaches and Molecular Simulation Research of the Intermolecular Interaction Between the Angiotensin-Converting Enzyme Inhibitor (ACE Inhibitor) Benazepril and Bovine Serum Albumin (BSA), *Spectrochim. Acta, Part A*, **212**: 15-24 (2019).

[34] Shi J.-H., Lou Y.-Y., Zhou K.-L., Pan D.-Q., Elucidation of Intermolecular Interaction of Bovine Serum Albumin with Fenhexamid: A Biophysical Prospect, *J. Photochem. Photobiol., B*, **180**: 125-133 (2018).

[35] Morris G.M., Goodsell D.S., Halliday R.S., Huey R., Hart W.E., Belew R.K., Olson A.J., Automated Docking Using a Lamarckian Genetic Algorithm and an Empirical Binding Free Energy Function, *J. Comput. Chem.*, **19(14)**: 1639-1662 (1998).

[36] Nasir Z., Shakir M., Wahab R., Shoeb M., Alam P., Khan R.H., Mobin M., Lutfullah, Co-precipitation Synthesis and Characterization of Co Doped SnO_2 NPs, HSA Interaction Via Various Spectroscopic Techniques and their Antimicrobial and Photocatalytic Activities, *International Journal of Biological Macromolecules*, **94**: 554-565 (2017).

[37] Shen G.-F., Liu T.-T., Wang Q., Jiang M., Shi J.-H., Spectroscopic and Molecular Docking Studies of Binding Interaction of Gefitinib, Lapatinib and Sunitinib with Bovine Serum Albumin (BSA), *J. Photochem. Photobiol., B*, **153**: 380-390 (2015).

[38] Yadav S., Yousuf I., Usman M., Ahmad M., Arjmand F., Tabassum S., Synthesis and Spectroscopic Characterization of Diorganotin (iv) Complexes of N′-(4-hydroxypent-3-en-2-ylidene) Isonicotinohydrazide: Chemotherapeutic Potential Validation by in Vitro Interaction Studies with DNA/HSA, DFT, Molecular Docking and Cytotoxic Activity, *RSC Adv.*, **5(63)**: 50673-50690 (2015).

[39] Nasir Z., Shakir M., Wahab R., Shoeb M., Alam P., Khan R.H., Mobin M., Co-Precipitation Synthesis and Characterization of Co Doped SnO_2 NPs, HSA Interaction Via Various Spectroscopic Techniques and their Antimicrobial and Photocatalytic Activities, *Int. J. Biol. Macromol.*, **94**: 554-565 (2017).

[40] Han X.-L., Tian F.-F., Ge Y.-S., Jiang F.-L., Lai L., Li D.-W., Yu Q.-L., Wang J., Lin C., Liu Y., Spectroscopic, Structural and Thermodynamic Properties of Chlorpyrifos Bound to Serum Albumin: A Comparative Study between BSA and HSA, *J. Photochem. Photobiol., B*, **109**: 1-11 (2012).

[41] Lakowicz J.R., Weber G., Quenching of Fluorescence by Oxygen. Probe for Structural Fluctuations in Macromolecules, *Biochemistry*, **12(21)**: 4161-4170 (1973).

[42] Wu, Li C., Hu Y., Liu Y., Study of Caffeine Binding to Human Serum Albumin Using Optical Spectroscopic Methods, *Sci. China, Ser. B: Chem.*, **52(12)**: 2205-2212 (2009).

[43] Rakotoarivelo N.V., Perio P., Najahi E., Nepveu F., Interaction between Antimalarial 2-Aryl-3 H-indol-3-one Derivatives and Human Serum Albumin, *J. Phys. Chem. B*, **118(47)**: 13477-13485 (2014).

[44] Fu Z., Cui Y., Cui F., Zhang G., Modeling Techniques and Fluorescence Imaging Investigation of the Interactions of an Anthraquinone Derivative with HSA and ctDNA, *Spectrochim. Acta, Part A*, **153**: 572-579 (2016).

[45] Ross P.D., Subramanian S., Thermodynamics of Protein Association Reactions: Forces Contributing to Stability, *Biochemistry*, **20(11)**: 3096-3102 (1981).

[46] Maltas E., Binding Interactions of Niclosamide with Serum Proteins, *J. Food Drug Anal.*, **4(22)**: 549-555 (2014).

[47] Buddanavar A.T., Nandibewoor S.T., Multi-Spectroscopic Characterization of Bovine Serum Albumin Upon Interaction with Atomoxetine, *J. Pharm. Anal.*, **7(3)**: 148-155 (2017).

[48] Oliveri V., Vecchio G., A Novel Artificial Superoxide Dismutase: Non-Covalent Conjugation of Albumin with A Mn III Salophen Type Complex, *Eur. J. Med. Chem.*, **46(3)**: 961-965 (2011).

[49] Lou Y.-Y., Zhou K.-L., Pan D.-Q., Shen J.-L., Shi J.-H., Spectroscopic and Molecular Docking Approaches for Investigating Conformation and Binding Characteristics of Clonazepam with Bovine Serum Albumin (BSA), *J. Photochem. Photobiol., B*, **167**: 158-167 (2017).

[50] Majidi S., Aramesh-Boroujeni Z., Moghadam M., Jahani S., Can One Novel Lanthanide Complex and Its Nano-Encapsulated Compounds Afford Advances in Biological Inorganic Chemistry? A Biological Applications Study for Dysprosium (III) Complex and Its Nano-Encapsulated Compounds, *Comments Inorg. Chem.*: 1-31 (2022).

[51] Jahani S., Aramesh-Boroujeni Z., Noroozifar M. *In vitro* Anticancer and Antibacterial Activates of the Yttrium(III) Complex and its Nano-Carriers toward DNA Cleavage and Biological Interactions with DNA and BSA; An Experimental and Computational Studies, *J. Trace Elem. Med. Biol.*, **68**: 126821 (2021).